Cell Research (2008) 18:458-471.

www.nature.com/cr

ORIGINAL ARTICLE

Redox status of thioredoxin-1 (TRX1) determines the sensitivity of human liver carcinoma cells ($HepG_2$) to arsenic trioxide-induced cell death

Changhai Tian[1], Ping Gao[1], Yanhua Zheng[3], Wen Yue[1], Xiaohui Wang[1], Haijing Jin[1], Quan Chen[1, 2]

[1]The Laboratory of Apoptosis and Cancer Biology, State Key Laboratory of Biomembrane and Membrane Biotechnology, Institute of Zoology, The Graduate School of Chinese Academy of Sciences, Chinese Academy of Sciences, Datun Rd, Chao Yang District, Beijing 100101, China; [2]College of Life Sciences, Nan Kai University, Tianjin 300071, China; [3]Department of Neuro-Oncology, MD Anderson Cancer Center, 1515 Holcombe Blvd., Houston, TX 77030, USA

Intracellular redox homeostasis plays a critical role in determining tumor cells' sensitivity to drug-induced apoptosis. Here we investigated the role of thioredoxin-1 (TRX1), a key component of redox regulation, in arsenic trioxide (As_2O_3)-induced apoptosis. Over-expression of wild-type TRX1 in $HepG_2$ cells led to the inhibition of As_2O_3-induced cytochrome c (cyto c) release, caspase activation and apoptosis, and down-regulation of TRX1 expression by RNAi sensitized $HepG_2$ cells to As_2O_3-induced apoptosis. Interestingly, mutation of the active site of TRX1 from $Cys^{32/35}$ to $Ser^{32/35}$ converted this molecule from an apoptotic protector to an apoptotic promoter. In an effort to understand the mechanisms of this conversion, we used isolated mitochondria from mouse liver and found that recombinant wild-type TRX1 could protect mitochondria from the apoptotic changes. In contrast, the mutant form of TRX1 alone elicited mitochondria-related apoptotic changes, including the mitochondrial permeability transition pore (mPTP) opening, loss of mitochondrial membrane potential, and cyto c release from mitochondria. These apoptotic effects were inhibited by cyclosporine A (CsA), indicating that mutant TRX1 targeted to mPTP. Alteration of TRX1 from its reduced form to oxidized form in vivo by 2,4-dinitrochlorobenzene (DNCB), a specific inhibitor of TRX reductase, also sensitized $HepG_2$ cells to As_2O_3-induced apoptosis. These data suggest that TRX1 plays a central role in regulating apoptosis by blocking cyto c release, and inactivation of TRX1 by either mutation or oxidization of the active site cysteines may sensitize tumor cells to As_2O_3-induced apoptosis.

Keywords: thioredoxin-1, arsenic trioxide, mitochondria, cytochrome c, apoptosis
Cell Research (2008) **18**:458-471. doi: 10.1038/cr.2007.112; published online 24 December 2007

Introduction

Arsenic trioxide (As_2O_3) has been used clinically to effectively treat acute promyelocytic leukemia (APL) [1, 2] and other types of cancers [3, 4]. This success prompts studies to investigate the molecular mechanisms of action underlying the clinic effectiveness. As_2O_3 might affect multiple intracellular signaling pathways, leading to alterations of cellular function. Subsequently, this compound was found to inhibit proliferation, or stimulate differentiation of tumor cells depending on the dosage and the cell system being used [5]. Increasing evidence has shown that As_2O_3 inhibits growth of APL cell lines and some solid tumors by inducing apoptosis [6, 7, 2]. As_2O_3 specifically induces degradation of a number of proteins including Bcl-2 and PML [8-10], thereby overcoming drug resistance even in the relapsed cancers. Also, As_2O_3 might target mitochondria to induce the opening of mitochondrial permeability transition pore (mPTP) [11, 12], thus increasing intracellular reactive oxygen species (ROS) generation, which could then lead to Bax conformational changes and its translocation [13]. These changes in mitochondrial physiology would result in cytochrome c (cyto c) release and subsequent activation

Correspondence: Quan Chen
Tel: +86 10 6480 7321
E-mail: chenq@ioz.ac.cn
Abbreviations**:** thioredoxin-1 (TRX1); cytochrome c (Cyto c); 4-acetamido-4′-maleimidylstilbene-2,2′-disulfonic acid (AMS); 2,4-dinitrochlorobenzene (DNCB); thioredoxin-2 (TRX2); mitochondrial permeability transition pore (mPTP); cyclosporine A (CsA)
Received 31 July 2007; revised 10 October 2007; accepted 30 October 2007; published online 24 December 2007

of the apoptotic cascade.

It is known that the intracellular redox system modulates both the anti-proliferative and pro-apoptotic effects of As_2O_3, and that the content of cellular GSH is negatively related to the sensitivity of tumor cells to As_2O_3 [14-16]. The redox state in mammalian cells is primarily a consequence of the precise balance between the level of ROS and endogenous thiol buffers present in the cell, particularly, GSH and thioredoxin (TRX), which protect cells from oxidative damage [17]. The role of GSH in protecting cancer cells from As_2O_3-induced apoptosis is well-documented [18]. GSH binds arsenic to form a transient As $(GS)_3$ complex, thereby preventing the inactivation of intracellular enzymes responsible for redox homeostasis. Thioredoxin-1 (TRX1) is a 12 kD ubiquitous protein having a redox-active disulfide/dithiol within the conserved active site sequence (-Cys-Gly-Pro-Cys-). Oxidized TRX1 with a disulfide on its active site is reduced by NADPH-dependent thioredoxin reductase1 (TR1) [19, 20] to restore its functions. TRX1 plays an important role in regulating cell redox homeostasis and cell growth, differentiation, and apoptosis. TRX1 inhibits cell apoptosis in a manner similar to that of Bcl-2 in the transfected cells. The mechanism for the inhibition of apoptosis by TRX1 has been suggested, whereby TRX1 could bind to and inhibit apoptosis signal-regulating kinase 1 (ASK1), thus regulating the JNK/p38 signaling pathway in response to environmental stresses such as ROS [21, 22]. The dissociation between TRX1 and ASK1 induced by ROS leads to the activation of the ASK1/JNK signaling pathway, and subsequent increase of apoptosis [23, 24]. Although TRX is regarded as a critical molecule for modulating cell death, its role in determining cancer cell sensitivity towards As_2O_3 has not been addressed. We thus attempted to investigate the role of cytoplasmic TRX1 in As_2O_3-induced apoptosis. Our results suggest that the redox status of TRX1 is important for modulating mitochondrial dependent apoptosis induced by As_2O_3. Inactivation of TRX1 either by mutation of the active site cysteine residues or by its oxidation enhances mitochondrial dependent apoptosis induced by As_2O_3. A better understanding of TRX1-mediated regulation of apoptosis elicited by As_2O_3 may offer novel targets for treating As_2O_3-resistant tumors and combinative drug therapy.

Results

TRX1 is involved in As_2O_3-induced apoptosis in $HepG_2$ cells

We used a clinically relevant concentration of As_2O_3 to treat the cell line $HepG_2$ at indicated times and then assayed apoptosis by examining Annexin V staining (data not shown) and the nuclear condensation. As_2O_3 induced apoptosis in a time-dependent manner in $HepG_2$ cells (Figure 1A and 1B). The optimal effect was obtained with 5 μM As_2O_3, with 45% cell death after 48 h treatment. Moreover, 5 μM As_2O_3 induced the release of cyto c in $HepG_2$ cells in a time-dependent manner (Figure 1C), concomitant of the onset of caspase activation (data not shown). These results suggest that As_2O_3 induced mitochondria-dependent apoptotic process as we described previously.

Human TRX1 acts as an important redox regulatory factor and plays a crucial role in drug-induced apoptosis [25]. We first examined the expression of TRX1 and found that the expression of TRX1 increased in a time-dependent manner in response to As_2O_3 treatment (Figure 1D), suggesting that TRX1 is involved in As_2O_3-induced apoptosis. To confirm that TRX1 is functionally important in the sensitivity of $HepG_2$ cells to As_2O_3, we performed RNA interference to specifically knock down the expression of TRX1 with oligonucleotides encoding short-hairpin RNAs (Ti108: 108-130nt and Ti214: 214-236nt). We found that Ti214 could effectively down-regulate the expression of endogenous TRX1 (Figure 2A). Treatment of Ti214-transfected $HepG_2$ cells with As_2O_3 resulted in a significant increase of apoptosis compared with untreated control cells, although extensive down-regulation of TRX1 alone appeared to increase Annexin V positive cells (Figure 2B). Down-regulation of TRX1 also augmented As_2O_3-induced cyto c release (Figure 2C). These data suggest that TRX1 regulates the As_2O_3-induced apoptosis in $HepG_2$ cells, perhaps via regulation of mitochondrial cyto c release.

TRX1 over-expression inhibits As_2O_3-induced apoptosis in $HepG_2$ cells

TRX1 over-expression is observed in many human primary cancers and appears to contribute to increased cell growth and a resistance to chemotherapy [26]. To further examine the effects of TRX1 on As_2O_3-induced apoptosis, we constructed recombinant adenoviruses expressing the wild-type TRX1 and mutant TRX1 ($cTm^{C32/35S}$) in which cysteine residues in the active site were changed to serine residues (see Figure 3A). We then analyzed the sensitivity of transfected $HepG_2$ cells to As_2O_3-induced apoptosis and found that over-expression of wild-type TRX1 could inhibit As_2O_3-induced apoptosis (Figure 3B). After As_2O_3 treatment for 24 h, the population of apoptotic cells in AdcTRX1-infected $HepG_2$ cells was reduced than that in AdGFP-infected cells or $AdcTm^{C32/35S}$-infected cells. To our surprise, the mutant form of TRX1 lost this protective effect, and over 55% cells were apoptotic in $AdcTm^{C32/35S}$-infected cells after As_2O_3 treatment for 12 h. These results indicate that the enzymatic activity of TRX1 was involved in susceptibility of $HepG_2$ cells to As_2O_3-induced apoptosis. Moreover, we noticed that $AdcTm^{C32/35S}$ alone could induce apoptosis in $HepG_2$ cells. Since it had been well established that cyto c release was a crucial event in As_2O_3-induced

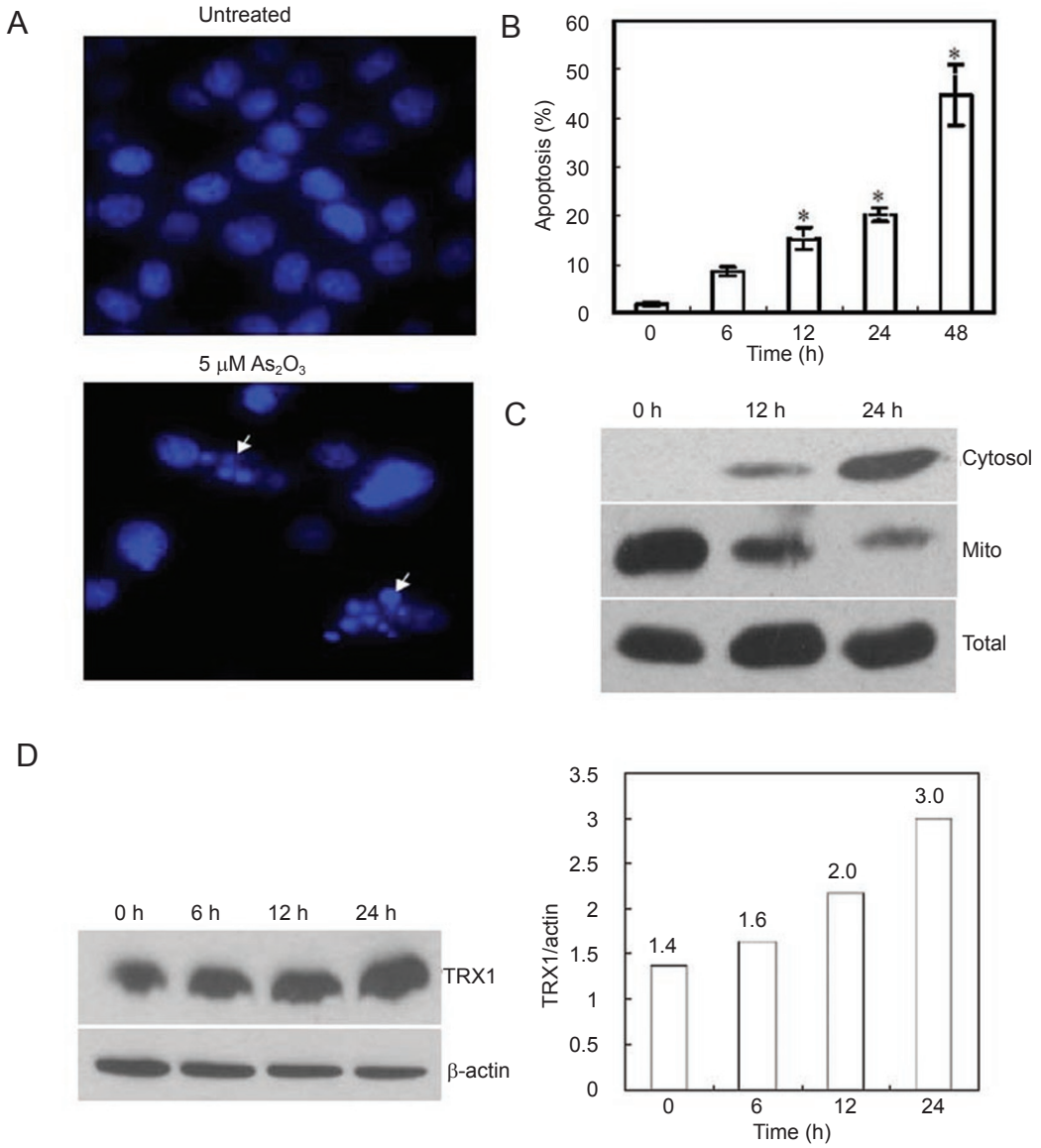

Figure 1 As_2O_3 induces apoptosis and TRX1 expression in $HepG_2$ cells. **(A, B)** Sensitivity of $HepG_2$ to As_2O_3-mediated apoptosis. $HepG_2$ cells were treated with 5 μM As_2O_3 for the indicated time, and then stained with Hoechst 33342. At least 200 apoptotic cells were counted in each experiment. Results are expressed as the mean ± SD for three independent determinations **(B**, panel right**)**, **P* < 0.05, compared with untreated cells. Apoptotic cells were characterized by nuclear condensation or fragmentation **(A**, left panel, bottom**)**. **(C)** As_2O_3 induces cyto c release from mitochondria to cytosol in $HepG_2$ cells in a time-dependent manner. Cells were exposed to 5 μM As_2O_3 for the indicated time, and then subjected to subcellular fractionation. Then, the cytosolic fraction (Cytosol) and mitochondrial fraction (Mito) were analyzed by immunoblotting (30 μg of protein per lane) with antibody specific for cyto c. **(D)** TRX1 expression after As_2O_3 treatment. Cells were treated with 5 μM As_2O_3 for indicated time, and then subjected to western blotting with antibodies specific for TRX1, β-actin as a loading control (panel left). The graph is the quantitative analysis of TRX1 expression with TotalLab v2.01 software (panel right).

apoptosis in APL cell lines [27, 28], we measured cyto c release and found that TRX1 could prevent cyto c release induced by As_2O_3, whereas $Tm^{C32/35S}$ lost its protective effect. Actually, the mutant form of TRX1 enhanced the cyto c release from mitochondria (Figure 3C).

We next transiently transfected $HepG_2$ cells with pcDNA3.1/Myc-His, recombinant pCDNA3.1-TRX1 and pCDNA3.1-$Tm^{C32/35S}$, and found that over-expression of wild-type TRX1 inhibited As_2O_3-induced caspase activation. In sharp contrast, over-expression of the mutant form

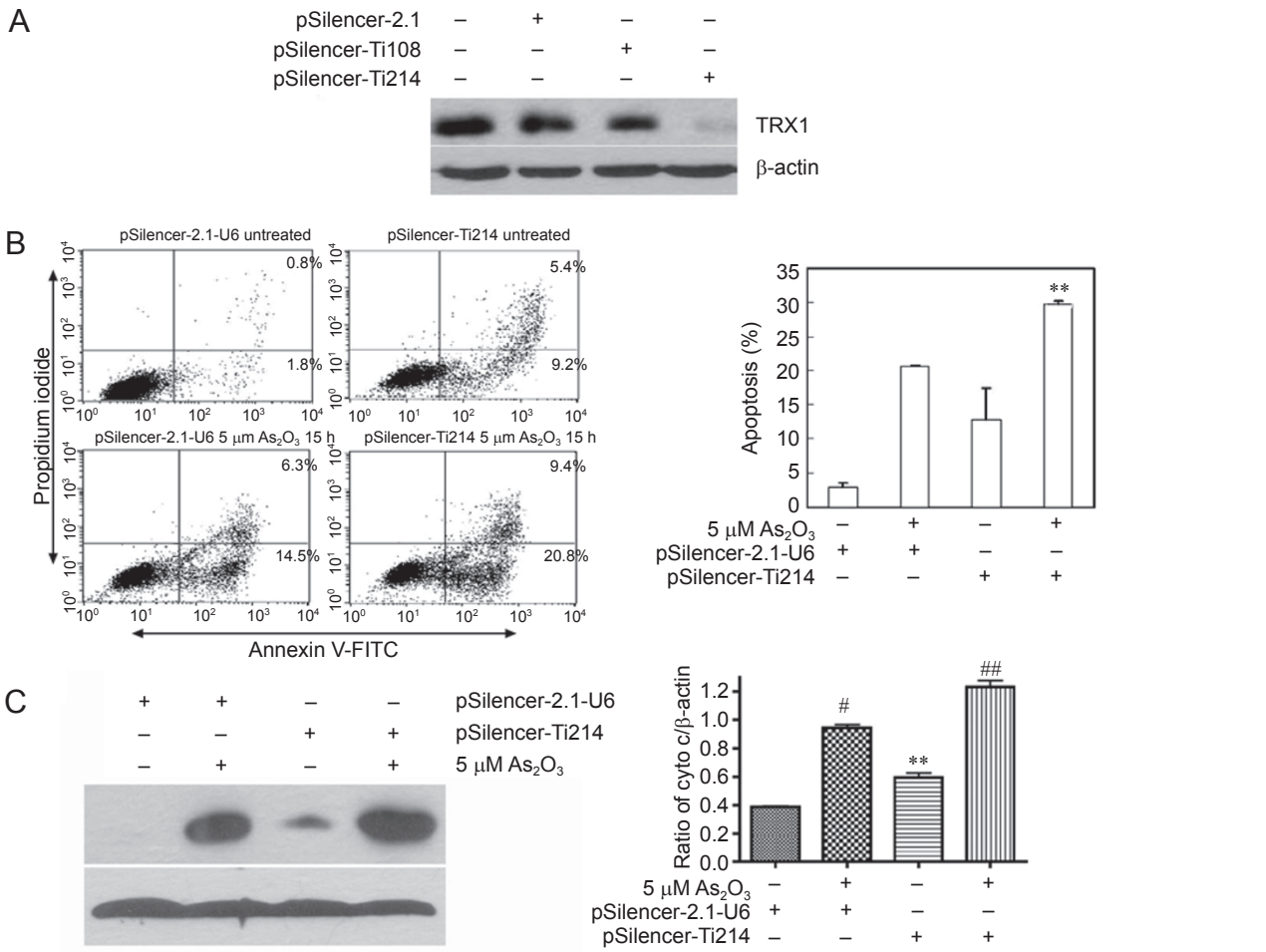

Figure 2 Vector-based RNAi specifically knocks down endogenous TRX1 expression and increases the cyto c release and apoptosis induced by As_2O_3. **(A)** $HepG_2$ cells were transiently transfected with RNAi expression vector pSilencer-sihTRX1 (Ti108, Ti214, 1 μg) or control vector pSilencer-2.1-U6 (1 μg). After 48 h post-transfection, endogenous TRX1 expression was determined by western blotting analysis with rabbit anti-human TRX1 polyclonal antibody, β-actin as a loading control. **(B)** $HepG_2$ cells were transiently transfected with pSilencer-Ti214 (1 μg) or pSilencer-2.1-U6 (1 μg), respectively. After 48 h, flow cytometric analysis of apoptosis in transfected cells treated in the presence or absence of 5 μM As_2O_3 for 15 h is performed by binding of Annexin V and uptake of PI. Apoptotic cells were defined as Annexin V positive. Results are expressed as mean ± SD for three independent experiments. $^{**}P < 0.01$ in comparison to As_2O_3-treated cells with pSilencer-2.1-U6. **(C)** The down-regulation of TRX1 in $HepG_2$ cells enhances the cyto c release. After 48 h, cells were exposed to 5 μM As_2O_3 for 15 h and subjected to subcellular fractionation. Then, the cytosolic fraction (Cytosol) was analyzed by immunoblotting (30 μg of protein per lane) with antibody specific for cyto c (upper panel); β-actin was used as a protein loading control (lower panel). Results were quantified as the ratio of cyto c to β-actin. Mean ± SD of three independent experiments was shown. $^{**}P < 0.01$ in comparison to cells transfected with pSilencer-2.1-U6; $^{\#}$denotes $P < 0.001$ in comparison to cells transfected with pSilencer-2.1-U6; $^{\#\#}$denotes $P < 0.001$ in comparison to cells transfected with pSilencer-2.1-U6 and treated with 5 μM As_2O_3.

$Tm^{C32/35S}$ enhanced caspase activation (Figure 3E). Taken together, these studies suggest that TRX1 regulates As_2O_3-induced apoptosis, at least in part, by a mechanism that involves its active site.

TRX1 prevents mitochondria-related apoptotic changes induced by As_2O_3, while TRX1 mutant promotes the changes in vitro

We next investigated the molecular mechanisms of how TRX1 regulates As_2O_3-induced apoptosis in its active site-dependent fashion. The recombinant human TRX1 (rTRX1) and its mutant ($rTm^{C32/35S}$) protein were expressed and purified, and these proteins were then used to treat the isolated mitochondria from mouse liver in the presence or absence of As_2O_3. In most cases 5 μM As_2O_3 was used, but in certain experiments, as indicated, to avoid potential damage to the mitochondria due to the prolonged exposure, higher dose (40 μM) and shorter duration of treatments

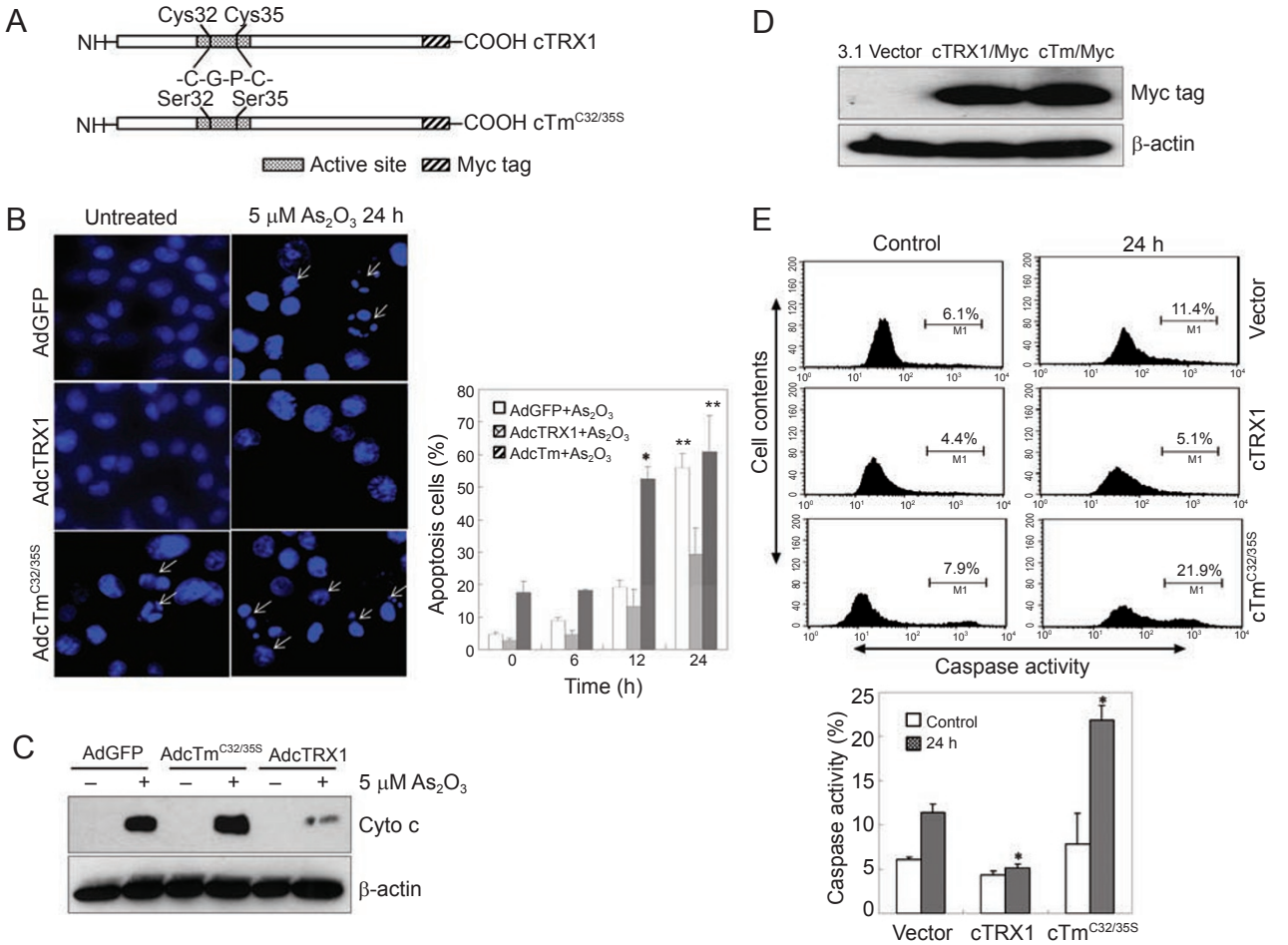

Figure 3 TRX1 protects $HepG_2$ cells against the As_2O_3-induced apoptosis through inhibiting cyto c release and caspase activation in an active-site dependent manner. **(A)** Diagram of wild-type, active site mutant of TRX1 with the c-terminal Myc tag represented as fancy diagonal boxes. The amino acid sequences for active site are enlarged. **(B)** Fluorescence micrographs of $HepG_2$ cells stained with Hoechst 33342. Cells infected with the recombinant adenovirus particles were treated with or without 5 μM As_2O_3 for 24 h. Cells were stained with Hoechst 33342 and numbered by fluorescence microscope. The apoptotic cells are characterized by nuclear condensation or fragmentation (left panel). The graph showed the percentage of apoptotic cells (n = 3, mean ± SD). *P < 0.05 in comparison to cells infected with AdGFP or AdcTRX1 which were treated with As_2O_3 for 12 h; **P < 0.01 in comparison to cells infected with AdcTRX1 and 24 h treatment with As_2O_3. **(C)** $HepG_2$ cells infected with the different recombinant adenovirus particles were treated with 5 μM As_2O_3 for 24 h before subcellular fractionation. The cytosolic fraction (Cytosol) was analyzed by immunoblotting (30 μg of protein per lane) with antibodies specific for cyto c, and using β-actin as a protein loading control. **(D)** Cells were transiently transfected with pCDNA3.1 (vector), pCDNA3.1-TRX1, and pCDNA3.1-$Tm^{C32/35S}$, respectively. After 48 h, the cells were collected and subjected to detection of TRX1 and $Tm^{C32/35S}$ expression with the antibody specific for Myc tag, β-actin as a loading control. **(E)** Cells transfected with recombinant plasmids were treated with 5 μM As_2O_3 for 24 h, then followed by incubation with FITC-VAD-fmk, a FITC-conjugated inhibitory substrate of caspase, and caspase activity analyzed by flow cytometry. The graph showed the statistical analysis results. *P < 0.05 in comparison to cells transfected with vector and treated with As_2O_3 for 24 h.

were applied. As expected, we found that rTRX1 could potently protect isolated mitochondria from swelling, an indicator of mPTP opening, induced by As_2O_3 (Figure 4A, traces c and d). As_2O_3 elicits the disruption of mitochondrial membrane potential, which is inhibited by rTRX1 (Figure 4B, trace d), similar to that of the PTP inhibitor, cyclosporine A (CsA) (Figure 4B, trace c). Surprisingly, $rTm^{C32/35S}$ alone could elicit mitochondrial swelling in a dose-dependent manner (Figure 4C, traces c, d, and e), and disrupt the mitochondrial membrane potential ($\Delta\psi_m$) in a dose-dependent manner (Figure 4C, traces b, c, and d). These effects were prevented by CsA, suggesting that $rTm^{C32/35S}$ could target the mPTP to evoke collapse of mitochondrial membrane potential. Our western blotting

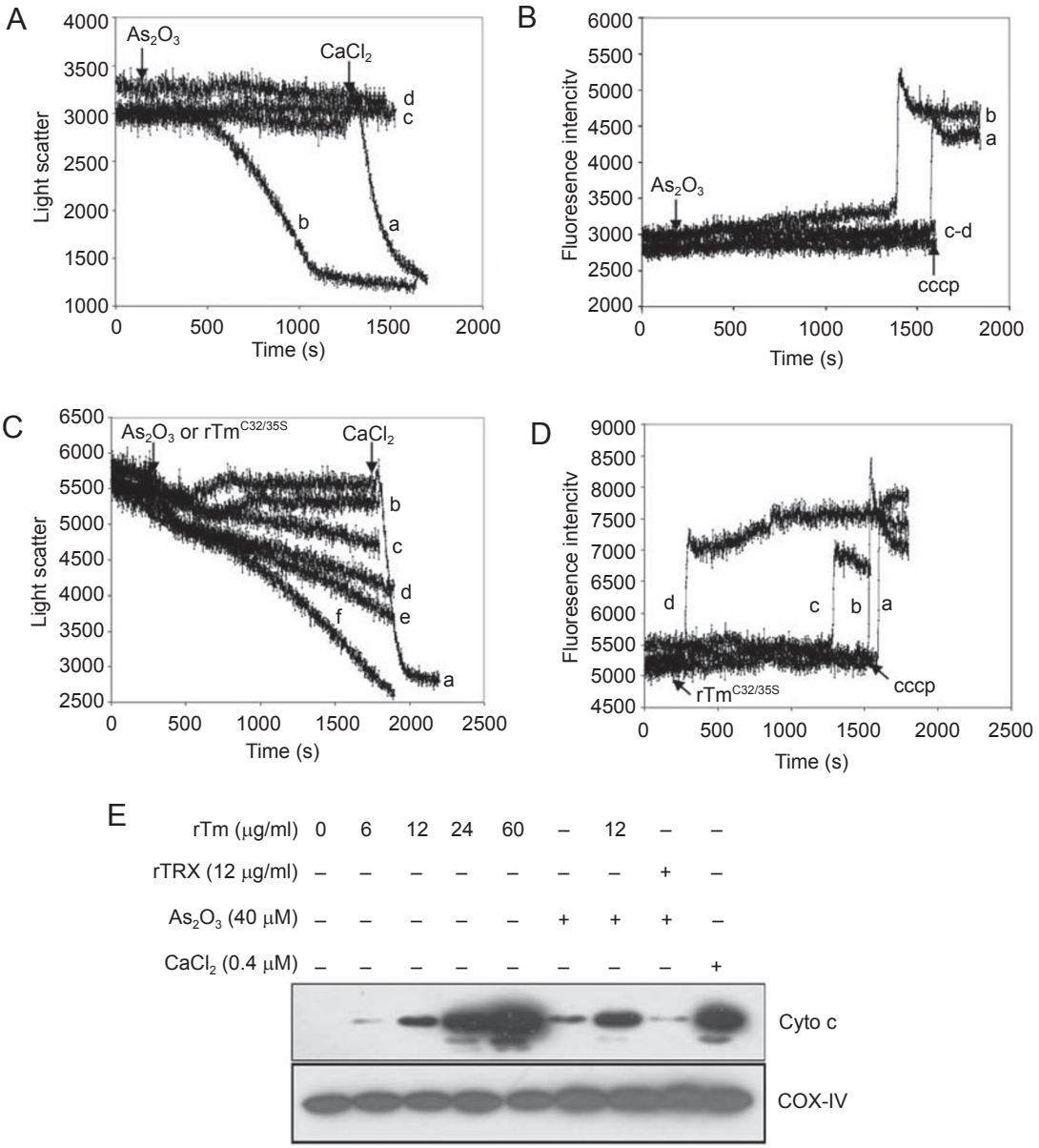

Figure 4 Purified rTRX1 regulates the apoptotic changes on the mitochondria level in an active site-dependent manner. Mitochondria swelling and $\Delta\Psi_m$ disruption induced by As_2O_3 were inhibited by PTP inhibitor and rTRX1. Isolated mitochondria (0.1 mg protein/ml) were incubated at 25 ºC in 3 ml PT-1 medium and were pretreated with different concentrations of rTRX1. **(A)** Trace a is control, $CaCl_2$ (added at 1 200 s) as positive control for mitochondrial swelling; Trace b is 40 μM As_2O_3; Trace c is 2 μg/ml rTRX1 plus 40 μM As_2O_3; Trace d is 4 μg/ml rTRX1 plus 40 μM As_2O_3. **(B)** Trace a is control, CCCP (added at 1 500 s) as positive control for the loss of mitochondrial membrane potential; Trace b is 40 μM As_2O_3; Trace c, 5 μM CsA plus 40 μM As_2O_3; Trace d, 4 μg/ml rTRX1 protein plus 40 μM As_2O_3. **(C)** Trace a, Control, $CaCl_2$ (added at 1800 s); Trace b, 8 μg/ml rTRX1; Trace c, 4 μg/ml $rTm^{C32/35S}$; Trace d, 8 μg/ml $rTm^{C32/35S}$; Trace e, 16 μg/ml $rTm^{C32/35S}$; Trace f, 40 μM As_2O_3. **(D)** Trace a, control, CCCP (added at 1600 s) as positive control; Trace b, 4 μg/ml $rTm^{C32/35S}$; Trace c, 8 μg/ml $rTm^{C32/35S}$; Trace d, 16 μg/ml $rTm^{C32/35S}$. Mitochondrial swelling **(A, C)** and $\Delta\Psi_m$ **(B, D)** were monitored by the decrease of 90° light scatter at 520 nm using a Jobin-Yvon FluoroMax-2 spectrofluorimeter or assessed by measuring the fluorescence intensity of the membrane potential dependent dye rhodamine 123 (30 nM) using a Jobin-Yvon FluoroMax-2 (excitation λ = 505 nm and emission λ = 534 nm), respectively. **(E)** Wild-type rTRX1 inhibited cyto c release from mitochondria induced by As_2O_3, $rTm^{C32/35S}$ enhanced the inductive effect of As_2O_3. Isolated mitochondria (1 mg protein/ml) were incubated for 60 min in 50 μl PT-1 medium with different concentrations of $rTm^{C32/35S}$ as indicated (panel left), isolated mitochondria were treated with As_2O_3, the combination of As_2O_3 and $rTm^{C32/35S}$ or rTRX1, $CaCl_2$ (0.4 μM) used as a positive control (panel right). The samples were then centrifuged at 12 000×*g* for 15 min at 4 °C. The levels of cyto c were measured by western blotting with an anti-cyto c antibody. Equal protein loading was confirmed by western blotting using the COX-IV antibody in the mitochondrial pellets.

analysis showed that rTRX1 inhibited the cyto c release induced by As_2O_3 (Figure 4E, panel right), whereas $rTm^{C32/35S}$ enhanced cyto c release in a dose-dependent manner (Figure 4E, panel left). Interestingly, $rTm^{C32/35S}$ alone, but not other mutant forms (C62S, C69S, and C73S, data not shown), induced cyto c release. These results further suggest that wild-type TRX1 may negatively regulate As_2O_3-induced apoptosis through the mitochondrial apoptotic pathway. Mutation of two cysteine residues to serine alters TRX1 function as assayed in mitochondria, suggesting that the redox activity of TRX1 is important for the regulation of As_2O_3-induced apoptosis.

Recombinant $Tm^{C32/35S}$ enhances ROS production and NAD(P)H oxidation in mitochondria

We next addressed how $rTm^{C32/35S}$ promotes mitochondrial changes. One possibility is that $rTm^{C32/35S}$ could translocate to mitochondria and perturb mitochondrial physiology, leading to mitochondrial dysfunction. It is well known that mitochondria are the major sources of superoxide and hydrogen peroxide in cells. Hence we examined whether rTRX1 and $rTm^{C32/35S}$ could target mitochondria. Following the incubation of isolated mitochondria with recombinant TRX1 and $rTm^{C32/35S}$, both rTRX1 and $rTm^{C32/35S}$ could be detected in mitochondrial membrane fractions (Figure 5A). We further examined the effects of $rTm^{C32/35S}$ on ROS production in isolated mitochondria. We used dischlorofluorescein (DCFH) to measure ROS production in mitochondrial matrix and found that $rTm^{C32/35S}$ increased the rate of ROS generation in isolated mitochondria, which was inhibited by recombinant Bcl-xL protein (Figure 5B) and CsA (data not shown). The levels of ROS were measured in the presence of succinate, so it is possible that ROS were produced by complex III in the respiratory chain, where the ratio of the reduced form versus oxidized form of NAD(P)H is an indicator of the redox potential in mitochondria. We thus examined the effects of $rTm^{C32/35S}$ on oxidation of NAD(P)H and found that $rTm^{C32/35S}$ induced NAD(P)H oxidation in mitochondria. Interestingly, we found that Bcl-xL potently inhibited the oxidation reaction (Figure 5C). These results suggest that $rTm^{C32/35S}$ may promote apoptosis through changing the mitochondrial redox balance, resulting in mPTP opening and cyto c release.

Oxidation of TRX1 abolishes the inhibitory effects of TRX1 on As_2O_3-induced apoptosis

Our above results suggest that the redox status of TRX1 is important to its function. It had been reported that, in the presence of oxidant, the active site loop forms part of the dimer interface and the activity of TRX1 may thus be blocked [29]. To confirm this, firstly, we used diamide as an oxidant to treat purified rTRX1 and observed the existent

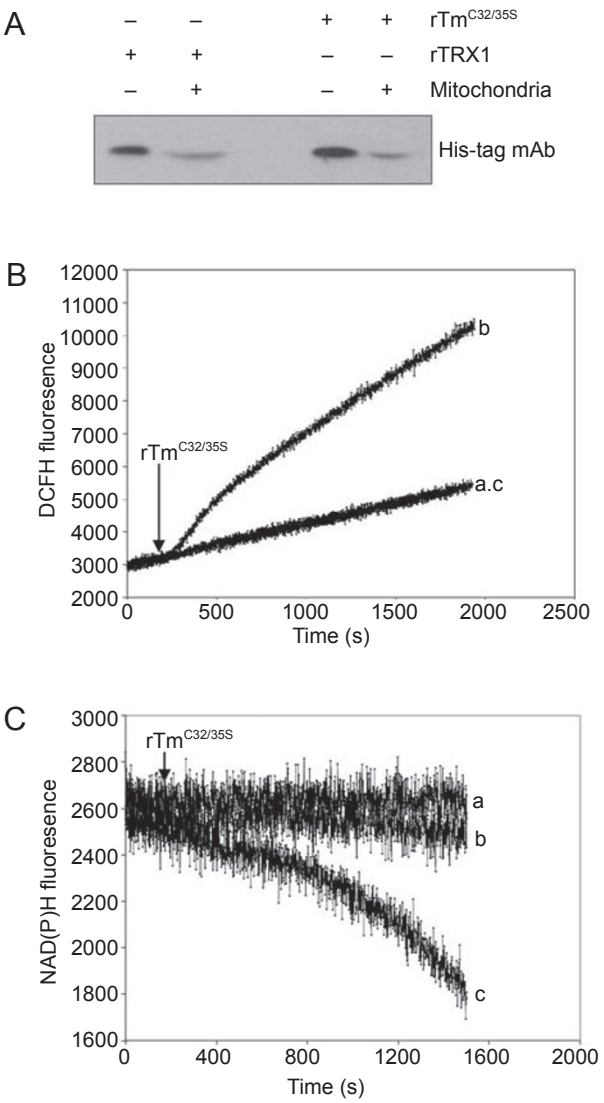

Figure 5 Recombinant $Tm^{C32/35S}$ enhances ROS production and NAD(P)H oxidation in mitochondria. **(A)** Membrane insertion of wild and mutant his-tagged rTRX1 onto mitochondria. Purified wild or mutant forms of rTRX1 were incubated with the isolated mouse liver mitochondria in respiration buffer for 30 min on ice, then centrifuged at 10 000×*g* for 15 min at 4 °C. Mitochondria pellets were washed with respiration buffer for three times, and then subjected to western blot analysis using anti-his tag monoclonal antibody. **(B)** $rTm^{C32/35S}$ induces an increase of mitochondrial ROS. ROS level was evaluated as described in Materials and Methods. Trace a is control; Trace b, 16 μg/ml $rTm^{C32/35S}$ was added at indicated time (arrow, 200 s); Trace c, Bcl-xL (20 μg/ml) was pre-incubated with the mitochondria before $rTm^{C32/35S}$ (16 μg/ml) was added as indicated. **(C)** The $rTm^{C32/35S}$ induces oxidation of NAD(P)H in mitochondria. The oxidation of NAD (P) H in mitochondria was measured as described in Materials and Methods. Trace a is control; Trace c, $rTm^{C32/35S}$ was added at indicated time (arrow, 200 s); Trace b, Bcl-xL (20 μg/ml) was preincubated with mitochondria before $rTm^{C32/35S}$ (16 μg/ml) was added (arrow).

forms of rTRX1 through non-reducing SDS-PAGE electrophoresis. Diamide induced the oligomerization of rTRX1 in a dose-dependent manner (Figure 6A). Moreover, we found that the oligomerization of rTRX1 not only altered its redox status (Figure. 6B), resulting in a decrease of the reduced form of rTRX1, but also led to the loss of its ability to inhibit As_2O_3-induced swelling in isolated mitochondrial (Figure 6C, trace c), and the failure to protect against As_2O_3-induced mitochondrial cyto c release (Figure 6D). These results further support our notion that the regulation of As_2O_3-induced apoptosis by TRX1 is dependent on its active site. An inactive form elicited by oxidant fails to protect mitochondria from swelling and cyto c release initiated by As_2O_3.

2,4-Dinitrochlorobenzene (DNCB) elicits the oxidization of TRX1, induces apoptosis and increases the sensitivity of $HepG_2$ cells to As_2O_3-induced apoptosis

Thioredoxin reductase (TR) is important for maintaining the reduced form of TRX1 in cells, and the inhibition of TR prevents the conversion of oxidized TRX1 into reduced form [30, 31]. We found that As_2O_3 could inhibit TR activity (data not shown), which is consistent with a previous report [32]. We treated $HepG_2$ cells with As_2O_3, DNCB (a specific inhibitor of TRX reductase) alone or the combination of both, then analyzed the redox status of TRX1 through non-reducing SDS-PAGE electrophoresis. Our results showed that TRX1 was oxidized by As_2O_3 and DNCB treatments in a time-dependent manner. The combination of As_2O_3 and DNCB induced significant increase in the oxidized

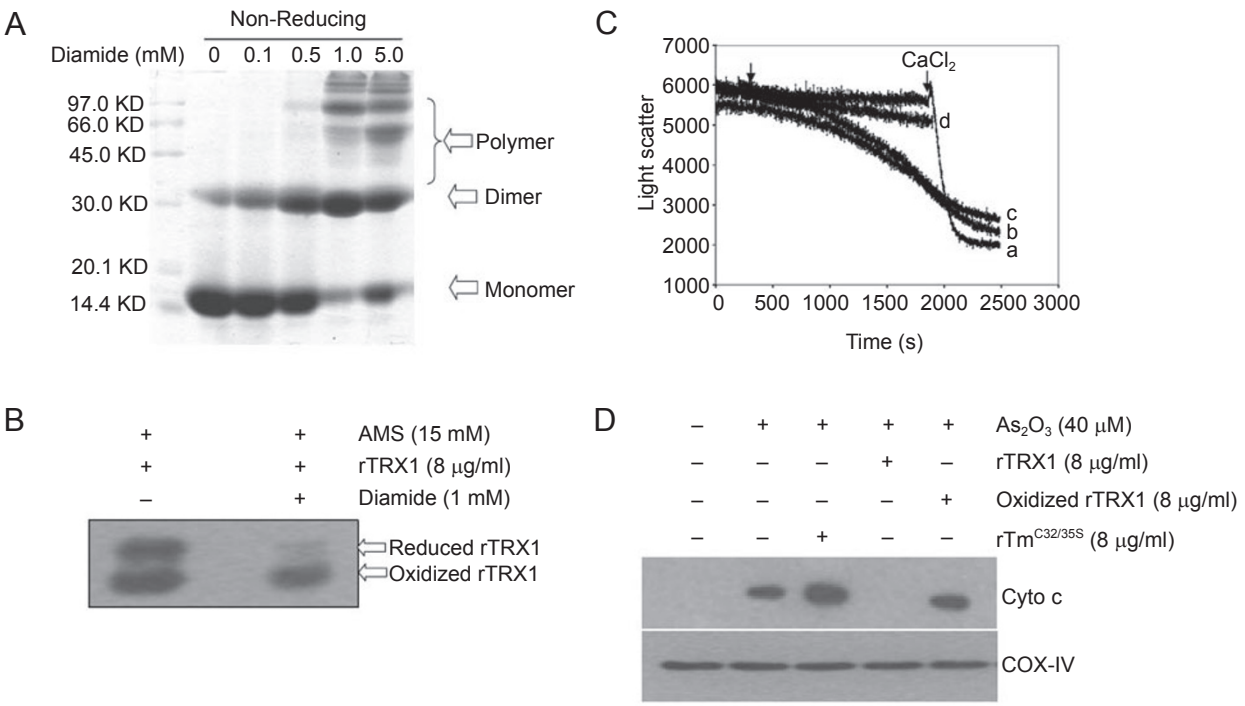

Figure 6 rTRX1 oxidization elicited by diamide fails to protect against As_2O_3-induced mitochondrial swelling and cyto c release. **(A)** Purified rTRX1 was treated with diamide as the indicated concentration, and then subjected to SDS-PAGE under non-reducing condition and stained with the Coomassie brilliant blue. **(B)** Determination of the redox status of rTRX1 [56]. Briefly, purified rTRX1 protein (1 μg/ml) was treated with or without 1 mM diamide, and was directly precipitated in 10% trichloroacetic acid (TCA). Precipitates were washed in 70% acetone and resuspended in 40 μl of reaction buffer (80 mM Tris-HCl, pH 6.8, 2% SDS) supplemented with a cocktail of protease inhibitors (Roche) and 15 mM freshly prepared AMS. Samples were incubated for 30 min at RT and for 10 min at 37 °C and then resolved by 15% SDS-PAGE. The redox state of TRX1 was detected by western blotting with anti-TRX1 antibody. **(C)** Isolated mitochondria were pre-incubated with 4 μg/ml oxidized rTRX1, then As_2O_3 was added at the indicated time (200 s). Trace a, Control ($CaCl_2$ added at 1 800 s); Trace b, 40 μM As_2O_3; Trace c, 8 μg/ml oxidized rTRX1 plus 40 μM As_2O_3; Trace d, 4 μg/ml rTRX1 plus 40 μM As_2O_3. Mitochondrial swelling was monitored as described in Materials and Methods. Data are representative of three independent experiments. **(D)** Isolated mitochondria (1 mg protein/ml) were pre-incubated with the oxidized rTRX1 or rTRX1, and then treated with the indicated concentration of As_2O_3. The release of cyto c was measured by western blotting with an anti-cyto c antibody, COX-IV in the mitochondrial pellets as a loading control.

form of TRX1 (Figure 7A). To further confirm whether the oxidization of TRX1 enhances As_2O_3-induced apoptosis in $HepG_2$ cells, we used a clinically relevant concentration of As_2O_3 (5 μM) to treat $HepG_2$ cells for 12 and 24 h in the presence or absence of DNCB, and then measured apoptosis with Annexin V and propidium iodide (PI) staining by flow cytometry. Our results showed that both As_2O_3 and DNCB induced an increase of Annexin V positive $HepG_2$ cells compared with control cells. The combination of both led to the greatest increase (11.5-fold) compared with control cells (Figure 7B). Moreover, the combination of As_2O_3 and DNCB significantly increased cyto c release from mitochondria (Figure 7C), consistent with caspase activation in a time-dependent manner (Figure 7D). These data indicate that the inhibition of TR activity by DNCB results in the oxidization of TRX1, and subsequently facilitates

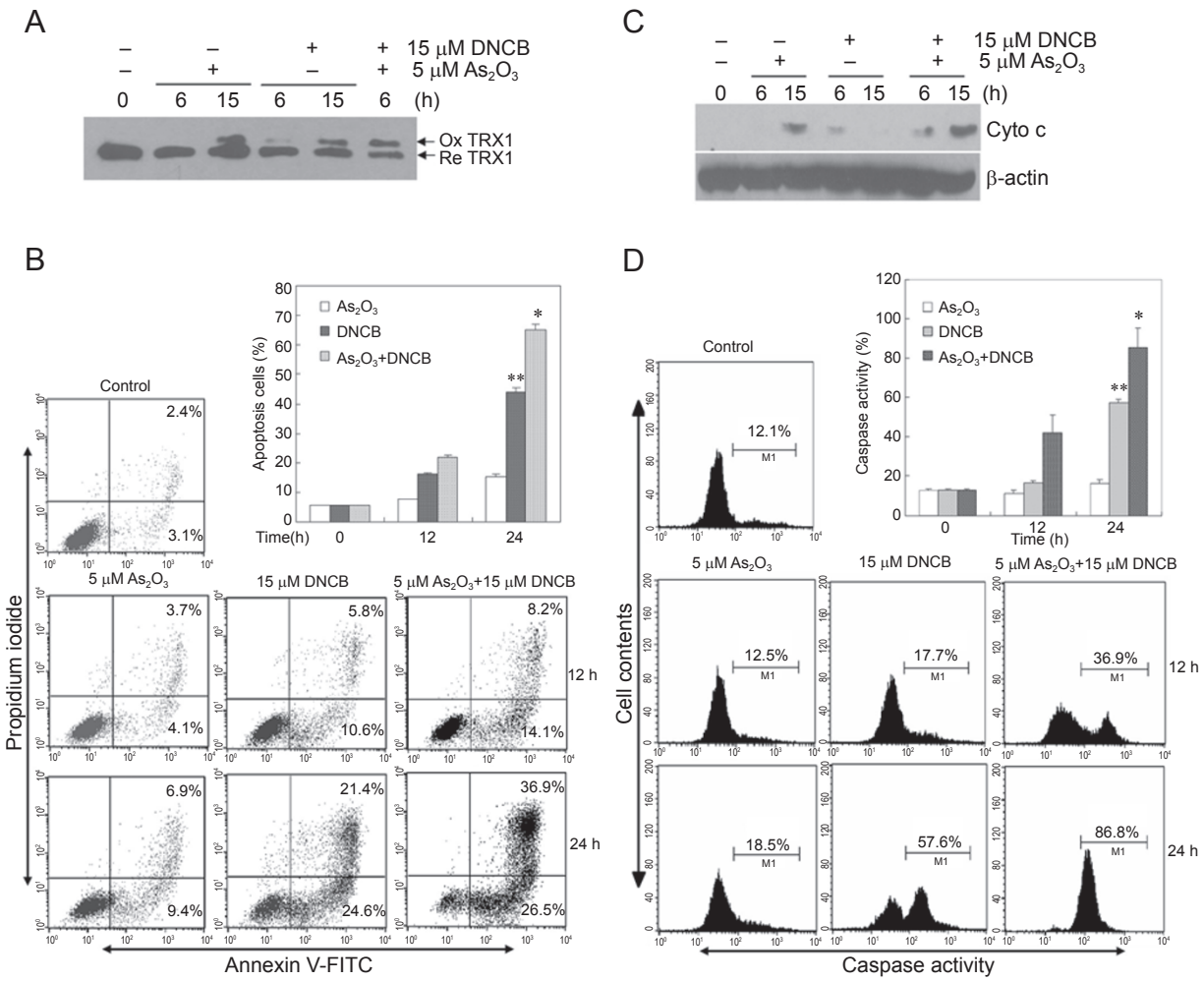

Figure 7 The alteration of TRX1 redox status increases the sensitivity of $HepG_2$ cells to As_2O_3-induced apoptosis. **(A)** As_2O_3 and DNCB could elicit the oxidation of TRX1. $HepG_2$ cells were treated with or without indicated concentrations of DNCB and As_2O_3 or the combination of both for the indicated time, then were directly precipitated in 10% TCA. Precipitates were resuspended in 40 μl reaction buffer and modified with 15 mM AMS at RT for 30 min, and then incubated at 37 °C for 10 min after washed twice in 70% acetone. Samples were resolved by 15% SDS-PAGE and detected by western blotting with TRX1 polyclonal antibody. **(B)** $HepG_2$ cells were treated with 5 μM As_2O_3 and 15 μM DNCB respectively or combinatively for 0, 12, 24 h; apoptotic cells were defined as Annexin V positive. The graph shows the statistical analysis results (n = 3, mean ± SD). $^{**}P < 0.01$ in comparison with untreated cells, $^{*}P < 0.05$ in comparison to cells treated with As_2O_3 or DNCB for 24 h. **(C)** $HepG_2$ cells were treated as indicated in **B**, and subjected to subcellular fractionation. Then, the cytosolic fraction (Cytosol) was analyzed by immunoblotting (30 μg of protein per lane) with antibodies specific for cyto c, β-actin as a loading control. **(D)** The caspase activity was detected as described in Materials and Methods. $HepG_2$ cells were treated as indicated, and then followed by incubation with FITC-VAD-fmk, a FITC-conjugated inhibitory substrate of caspase, and analyzed by flow cytometry. The graph showed the statistical analysis results ($n = 3$, mean ± SD). $^{**}P < 0.01$ in comparison to untreated cells; $^{*}P < 0.05$ in comparison to cells treated with As_2O_3 or DNCB for 24 h.

As_2O_3-induced apoptosis.

Discussion

In this study, we showed the critical role of TRX1 in regulating As_2O_3-induced apoptosis. First, the expression level of TRX1 in cells is important for regulating cell death and drug sensitivity. Increased expression of wild-type TRX1 prevents $HepG_2$ cells from As_2O_3-induced apoptosis, while down-regulation of TRX1 with RNAi sensitizes the cells towards As_2O_3-induced apoptosis. Second, we found that the redox status of TRX1 determines the sensitivity of $HepG_2$ cells to As_2O_3 treatment. Mutation of the active site cysteines in TRX1 enhanced As_2O_3-induced apoptosis. *In vitro* oxidization of TRX1 also caused a lost of protective function. To further support this notion, we found that DNCB, a specific inhibitor of TR, could induce TRX1 oxidation and significantly sensitized cells to As_2O_3-induced apoptosis. Previous studies have shown that arsenic can react with cysteine residues of GSH or TR to inactivate intracellular enzymes responsible for redox homeostasis [33, 34]. Our results also suggest a novel mechanism for sensitizing cancer cells to As_2O_3-induced apoptosis by modulating TRX1 redox status. This can be achieved either by inhibiting TR activity (Figure 7) or by direct reactions with cysteine residues within the TRX1 active site.

The redox status of TRX1 could also affect its interaction with ASK1, or other important molecules which mediate cell apoptosis [35]. However, our findings of this study suggest that mutation of the TRX1 active site cysteines could directly elicit destabilization of mitochondrial bioenergetics as well as cyto c release in the cells and isolated mitochondria, while wild-type TRX1 could prevent the apoptotic effects induced by both mutant TRX1 and As_2O_3. Direct application of the mutant form of TRX1 (C32S/35S), but not other mutant forms, to isolated mitochondria elicited the opening of mPTP, the loss of $\Delta\psi_m$, and subsequently the release of cyto c. Similarly, the oxidized form of TRX1 lost its function as an anti-apoptosis molecule and was able to enhance the apoptotic catastrophe of mitochondria. These effects appear to be direct in our *in vitro* system, without the involvement of cytosolic factors or signaling pathways as reported previously. Since TRX1 acts as one of the key components in the antioxidant system which antagonizes oxidative stress-induced apoptosis [35, 36], our work supports that inactivation of TRX1 would confer a therapeutic advantage to cancer treatment by targeting mitochondria.

Questions remain regarding how inactivation or mutation of TRX1 directly elicits a mitochondria-related apoptotic response. We found that mutant TRX1 could disturb the redox potential of mitochondria as it caused the oxidation of mitochondrial NADH/NADPH and increased ROS production. This may subsequently perturb the mitochondrial redox pool of GSH and mtTRX2 (mitochondrial thioredoxin-2 (TRX2)), which are substrates of mitochondrial glutathione peroxidase and thioredoxin peroxidase, and thus decrease the capacity of these enzymes to remove H_2O_2. The perturbation of the redox pool may then globally modulate the mitochondria physiology, resulting in the opening of mPTP and increase of ROS production [37]. In addition, it has also been shown that cyto c that is released from mitochondria is a potent catalyst of DCFH oxidation [38], and DCF fluorescence observed in the presence of $rTm^{C32S/35S}$ may be a reflection of increased cyto c content in the incubation buffer. This is unlikely in our system since this dye measured the ROS in the mitochondrial matrix. To support these notions, we found that DTT, NADH, and ROS scavengers prevented $rTm^{C32S/35S}$-induced mitochondria-related apoptotic changes (unpublished data). Another possibility is that the insertion of recombinant TRX1 proteins into the mitochondria and interactions with VDAC1 or other molecules modulate PTP activity for cyto c release. Our results were consistent with a previous report which proved the interaction between TRX1 and VDAC1 [39], since our pull-down assay showed that TRX1 could interact with VDAC1 in our system (data not shown). One report indicates that mitochondrial TRX2 might directly regulate cyto c release through the physical interaction with cyto c in mitochondria [40]. It remains to be determined if TRX1 can interact with cyto c.

In summary, our results indicate that TRX1 regulates As_2O_3-induced apoptosis by preventing mitochondrial cyto c release. Inactivation of TRX1 either by mutation of the active cysteine residues or by oxidation enhances mitochondria-dependent apoptosis induced by As_2O_3. Further studies are required to develop strategies to enhance the effect of As_2O_3 therapy by modulating TRX1 activity *in vivo*.

Materials and Methods

Materials

Arsenic trioxide (A-1010) was purchased from Sigma (St. Louis, MO); 4-acetamido-4′-maleimidylstilbene-2,2′-disulfonic acid, disodium salt (AMS) (A-485), and anti-cyto c oxidase monoclonal antibody (subunit IV) were from Molecular Probes (Eugene, OR). ProBondTM metal affinity Resin was purchased from Invitrogen (San Diego, CA), and Amicon®Ultra-15 concentrator was from Millipore (Billerica, MA). Anti-cyto c mouse monoclonal antibody was from BD Biosciences Pharmingen (San Jose, CA). Rabbit anti-human thioredoxin polyclonal IgG1 (sc-20146) was from Santa Cruz Biotechnology (Santa Cruz, CA). All other chemicals were purchased from Sigma (St. Louis, MO).

Cell culture and transfection

Human embryonic kidney 293A (HEK293A) cells, purchased from the Cell Bank of the Chinese Academic of Sciences (Shanghai, China), were maintained in Dulbecco's modified Eagle's medium (GIBCO); human hepatoma $HepG_2$ cells (from ATCC) were main-

tained in 1640 medium, both supplemented with 10% (v/v) fetal bovine serum (HyClone), 100 μg/ml streptomycin and 100 U/ml penicillin (HyClone) at 37 ºC in humidified 5% CO_2 atmosphere. Cell transfection was performed as described in the LIPOFECAMINE™ Reagent (GIBCO) manual.

Detection of cell death by Hoechst 33342 and Annexin-V-FITC

For Hoechst 33342 staining, cells were plated at low density on glass coverslides in a six-well plate and treated with 5 μM As_2O_3. After indicated time, cells were stained with Hoechst 33342 in PBS (15 min at room temperature in the dark). Cells were then washed three times with PBS and analyzed under a fluorescence microscope, and at least 200 cells were counted. Apoptotic cells were detected by flow cytometry. Phosphatidylserine exposed on the outside of the cells was determined by Annexin V-FITC kit. Briefly, $HepG_2$ cells were plated in six-well plates and treated with As_2O_3 for the indicated time. At the end of the experiment, cells were digested with trypsin-EDTA solution, then collected by centrifugation and washed twice with ice-cold PBS. After being washed one more time with the incubation buffer (10 mM HEPES/NaOH, pH 7.4, 140 mM NaCl, and 5 mM $CaCl_2$), cells were stained with Annexin V-FITC and PI for 20 min in dark at room temperature; then an additional 400 μl binding buffer was added before FACS analysis [41]. Flow cytometric analysis was performed to monitor the green fluorescence of the FITC-conjugated Annexin V (530±30 nm) and the red fluorescence of DNA-bound PI (630±22 nm). All data were analyzed with Cell Quest software (BD).

SDS-PAGE and immunoblotting

SDS-PAGE and immunoblotting were performed as described elsewhere [42]. Briefly, the cells or membrane fractions were resuspended in NP-40 containing lysis buffer (10 mM HEPES (pH 7.4), 2 mM EGTA, 0.5% NP-40, 1 mM NaF, 1 mM $NaVO_4$, 1 mM phenylmethylsulfonyl fluoride (PMSF), 1 mM DTT, 50 mg/ml trypsin inhibitor, 10 mg/ml aprotinin, and leupeptin) and placed on ice for 30 min. The lysates were centrifuged at 12 000×*g* for 12 min at 4 °C, and the protein concentration was determined with BSA as a standard. Equivalent samples (30 μg protein) were subjected to SDS-PAGE on 12% gel. The proteins were then transferred onto nitrocellulose membranes, and probed with the indicated antibodies followed by the appropriate secondary antibodies conjugated to horseradish peroxidase (KPL, Gaithersburg, MD, USA). Immunoreactive bands were visualized using enhanced chemiluminescence (Pierce). The molecular sizes of the developed proteins were determined by comparison with prestained protein markers (Invitrogen, Carlsbad, CA, USA).

Cell fractionation

As_2O_3-treated cells were fractionated by differential centrifugation as described previously[43-45]. Briefly, cells were harvested through trypsin digestion, and then centrifuged and resuspended in three volumes of hypotonic buffer (210 mM sucrose, 70 mM mannitol, 10 mM HEPES (pH 7.4), 1 mM EDTA) containing 1 mM PMSF, 50 mg/ml trypsin inhibitor, 10 mg/ml leupeptin, 5 mg/ml aprotinin and 10 mg/ml pepstatin. After gentle homogenization with a Dounce homogenizer, cell lysates were centrifuged at 1 000×*g* for 5 min to remove unbroken cells and nuclei and the cytosolic fractions were obtained by further centrifugation at 10 000×*g* for 30 min.

Generation of adenoviral recombinants and plasmids construction

The adenoviral recombinants of Ad-cTRX1 and Ad-$cTm^{C32/35S}$ were generated according to previous methods [46]. Briefly, PCR products (Bgl II + Not I) of TRX1 and its mutant were subcloned into pAdTrack-CMV shuttle vector. Recombinant adenoviral plasmids were generated by homologous recombination of recombinant shuttle vector linearized with PmeI and AdEasy-1 in *BJ5183 Escherichia coli* cells. Then, the recombinant adenovirus plasmids were linearized with PacI and then transfected into HEK293A cells to package recombinant virus. Virus propagation and amplification were then achieved by standard techniques.

To generate the over-expression of cTRX1 and $cTm^{C32/35S}$ vector, their cDNA fragments were subcloned into pCDNA3.1/myc-his vector and were confirmed by sequencing. In addition, to generate TRX1 RNAi vector, one annealed set of oligonucleotides encoding short-hairpin transcripts corresponding to nt 108-130 (named Ti108) and 214-236 (named Ti214) of human TRX1 mRNA (GenBank accession no. AF276919) were cloned into pSilencer-2.1-U6 (Ambion; hereafter abbreviated to pSilencer). In brief, the short-hairpin-RNA-encoding complementary single-stranded oligonucleotides, which hybridized to give overhangs compatible with *Bam*HI and *Hin*dIII, were designed with a computer program available on the internet *http://www.ambion.com/techlib/misc/psilencer_converter.html.* Oligonucleotides encoding short-hairpin RNAs were then ligated into pSilencer. The positive clones were confirmed by sequencing.

Expression and purification of recombinant proteins

The recombinant proteins were expressed and purified as described previously [47]. Briefly, His-tagged human TRX1 and $Tm^{C32/35S}$ were obtained through subcloning into the pET-28a (+). The resulting plasmids were transformed into *E. coli* BL21 (DE3). The positive transformants were induced for 4 h at 25 ºC by the addition of 1 mM isopropyl-b-D-thiogalactopyranoside (IPTG; Sigma). The induced cells were pelleted, resuspended in native binding buffer (20 mM sodium phosphate, 500 mM sodium chloride, pH 7.8), sonicated on ice, and centrifuged at 4 ºC for 30 min at 30 000×*g* to remove cell debris. The supernatants containing fusion proteins were purified with ProBond™ metal affinity resin and concentrated with Amicon® Ultra-15 concentrators. The protein purity was verified by 12% SDS-PAGE and stained with Coomassie brillant blue R-250. The protein concentration was determined with BSA as a standard.

Isolation of mouse liver mitochondria and measurement of PTP opening and mitochondrial membrane potential ($\Delta\psi_m$)

Liver mitochondria from Balb/c mice were isolated by method as described previously [48-50]. Briefly, mice livers were homogenized with a glass-Teflon Potter homogenizer. Samples were centrifuged at 4 ºC, 1 000×*g* for 10 min. Then the supernatant was transferred to another tube and centrifuged at 4 ºC, 10 000×*g* for 10 min. Mitochondria were washed twice, then resuspended in the same medium. Isolated mitochondria (5 mg protein/ml) were kept in MT buffer containing 250 mM sucrose, 2 mM HEPES, pH 7.4, 0.1 mM EDTA, and 0.1% fatty acid-free BSA. PTP opening was monitored by the decrease of 90° light scattering at 520 nm at 25 ºC in medium PT-1 containing 250 mM sucrose, 2 mM HEPES, pH 7.4, 0.5 mM KH_2PO_4, 2 mM rotenone, and 4.2 mM potassium succinate, using a Jobin Yvon FluoroMax-2 spectrofluorimeter as described [51].

In addition, determination of mitochondrial membrane potential ($\Delta\psi_m$) was performed as described previously[52, 53]. Briefly, after addition of 30 nM Rh123 to a mitochondria suspension, Dym was assessed at 25 ºC in medium PT-1 by measuring the uptake of Rh123 using a spectrofluorimeter (Jobin Yvon FluoroMax-2).

Assay of ROS production and determination of the NAD(P)H redox state

The generation of mitochondrial ROS was evaluated in isolated mitochondria in medium PT-1 using DCFH as a probe as described previously[54]. DCF formation was monitored using a Jobin Yvon FluoroMax-2 spectrofluorimeter. The oxidation of NAD(P)H in the mitochondria was measured at excitation and emission wavelengths of 350 and 450 nm as described [55]. All assays were carried out in triplicate.

Cyto c release and western blot analysis

Mouse liver mitochondria were isolated following the above method and protein content of isolated mitochondria was determined by the micro-biuret method using BSA as a standard. Equal mitochondria fractions were treated with different concentrations of $rTm^{C32/35S}$ at 25 ºC in PT-1 buffer for 60 min; in addition, 12 μg/ml rTRX1 was pre-incubated with mitochondria for 10 min, then 12 μg/ml $rTm^{C32/35S}$ and 40 μM arsenic trioxide was added and incubated for the same time. The samples were then centrifuged at 12 000×*g* for 15 min at 4 ºC. Cyto c resulting from the supernatant was detected by western blotting using anti-cyto c monoclonal antibody and visualized by ECL Supersignal system (Pierce), and equal protein loading was confirmed by immunodetection of cyto c oxidase subunit IV (COX-IV) in the mitochondrial pellets. The sample treated with 0.4 μM $CaCl_2$ was a positive control as indicated.

Detection of caspase activation in situ

The method was performed following the CaspACE™ FITC-VAD-FMK *in situ* Marker kit manual. Briefly, cells were digested with trypsin-EDTA solution, then collected and washed with PBS. CaspACE™ FITC-VAD-FMK *In situ* Marker was added to the cells at a final concentration of 10 μM, and then incubated for 20 min in the dark. Cells were washed three times with PBS, and resuspended in 400 μl PBS and measured with a FACScan.

Statistical analysis

Significant differences between values under different experimental conditions were determined by paired Student *t* test analyses. A value of $P<0.05$ was considered to be significant.

Acknowledgments

We are grateful to Dr Maryam Mehrpour (Laboratoire de Cytokines et Immunologie des tumeurs Humaines, Institut Gustave Roussy PR1 and IFR 54, Villejuif, France) and Nathan B Erdmann (Department of Pharmacology and Experimental Neuroscience and Pathology and Microbiology, University of Nebraska Medical Center, Omaha, NE, USA) for their thoughtful comments. We wish to thank Dr Junji Yodoi (Department of Biological Responses, Institute for Virus Research, Kyoto University, Japan) for his generous provision of thioredoxin mutant plasmid, and Mrs Jing Wang for her technical assistance in flow cytometry. This work was supported by grants from the National Proprietary Basic Research Program (973 program project, Nos. 2002CB513100 and 2004CB72000), and a National Outstanding Young Investigator Fellowship (No.30325013) from NSFC awarded to Chen Q.

References

1 Shen ZX, Chen GQ, Ni JH, *et al*. Use of arsenic trioxide (As2O3) in the treatment of acute promyelocytic leukemia (APL): II. Clinical efficacy and pharmacokinetics in relapsed patients. *Blood* 1997; **89**:3354-3360.

2 Chen GQ, Zhu J, Shi XG, *et al*. In vitro studies on cellular and molecular mechanisms of arsenic trioxide (As2O3) in the treatment of acute promyelocytic leukemia: As2O3 induces NB4 cell apoptosis with downregulation of Bcl-2 expression and modulation of PML-RAR alpha/PML proteins. *Blood* 1996; **88**:1052-1061.

3 Kong B, Huang S, Wang W, *et al*. Arsenic trioxide induces apoptosis in cisplatin-sensitive and -resistant ovarian cancer cell lines. *Int J Gynecol Cancer* 2005; **15**:872-877.

4 Xie D, Yin S, Ou Y, *et al*. Arsenic trioxide (As(2)O(3)) induced apoptosis and its mechanisms in a human esophageal squamous carcinoma cell line. *Chin Med J* 2002; **115**:280-285.

5 Miller WH Jr, Schipper HM, Lee JS, Singer J, Waxman S. Mechanisms of action of arsenic trioxide. *Cancer Res* 2002; **62**:3893-3903.

6 Zhang TC, Cao EH, Li JF, Ma W, Qin JF. Induction of apoptosis and inhibition of human gastric cancer MGC-803 cell growth by arsenic trioxide. *Eur J Cancer* 1999; **35**:1258-1263.

7 Chen Z, Wang ZY, Chen SJ. Acute promyelocytic leukemia: cellular and molecular basis of differentiation and apoptosis. *Pharmacol Ther* 1997; **76**:141-149.

8 Shen ZX, Shi ZZ, Fang J, *et al*. All-trans retinoic acid/As2O3 combination yields a high quality remission and survival in newly diagnosed acute promyelocytic leukemia. *Proc Natl Acad Sci USA* 2004; **101**:5328-5335.

9 Mahieux R, Pise-Masison C, Gessain A, *et al*. Arsenic trioxide induces apoptosis in human T-cell leukemia virus type 1- and type 2-infected cells by a caspase-3-dependent mechanism involving Bcl-2 cleavage. *Blood* 2001; **98**:3762-3769.

10 Quignon F, De BF, Koken M, Feunteun J, Ameisen JC, de TH. PML induces a novel caspase-independent death process. *Nat Genet* 1998; **20**:259-265.

11 Tian X, Ma X, Qiao D, Ma A, Yan F, Huang X. mCICR is required for As2O3-induced permeability transition pore opening and cytochrome c release from mitochondria. *Mol Cell Biochem* 2005; **277**:33-42.

12 Zheng Y, Shi Y, Tian C, *et al*. Essential role of the voltage-dependent anion channel (VDAC) in mitochondrial permeability transition pore opening and cytochrome c release induced by arsenic trioxide. *Oncogene* 2004; **23**:1239-1247.

13 Zheng Y, Yamaguchi H, Tian C, *et al*. Arsenic trioxide (As(2)O(3)) induces apoptosis through activation of Bax in hematopoietic cells. *Oncogene* 2005; **24**:3339-3347.

14 Maeda H, Hori S, Ohizumi H, *et al*. Effective treatment of advanced solid tumors by the combination of arsenic trioxide

and L-buthionine-sulfoximine. *Cell Death Differ* 2004; **11**:737-746.
15 Zhou L, Jing Y, Styblo M, Chen Z, Waxman S. Glutathione-S-transferase pi inhibits As2O3-induced apoptosis in lymphoma cells: involvement of hydrogen peroxide catabolism. *Blood* 2005; **105**:1198-1203.
16 Lu M, Xia L, Luo D, Waxman S, Jing Y. Dual effects of glutathione-S-transferase pi on As2O3 action in prostate cancer cells: enhancement of growth inhibition and inhibition of apoptosis. *Oncogene* 2004; **23**:3945-3952.
17 Davis W Jr, Ronai Z, Tew KD. Cellular thiols and reactive oxygen species in drug-induced apoptosis. *J Pharmacol Exp Ther* 2001; **296**:1-6.
18 Jing Y, Dai J, Chalmers-Redman RM, Tatton WG, Waxman S. Arsenic trioxide selectively induces acute promyelocytic leukemia cell apoptosis via a hydrogen peroxide-dependent pathway. *Blood* 1999; **94**:2102-2111.
19 Nakamura H, Nakamura K, Yodoi J. Redox regulation of cellular activation. *Annu Rev Immunol* 1997; **15**:351-369.
20 Holmgren A. Thioredoxin. *Annu Rev Biochem* 1985; **54**:237-271.
21 Tobiume K, Matsuzawa A, Takahashi T, *et al*. ASK1 is required for sustained activations of JNK/p38 MAP kinases and apoptosis. *EMBO Rep* 2001; **2**:222-228.
22 Matsuura H, Nishitoh H, Takeda K, *et al*. Phosphorylation-dependent scaffolding role of JSAP1/JIP3 in the ASK1-JNK signaling pathway. A new mode of regulation of the MAP kinase cascade. *J Biol Chem* 2002; **277**:40703-40709.
23 Li X, Zhang R, Luo D, *et al*. Tumor necrosis factor alpha-induced desumoylation and cytoplasmic translocation of homeodomain-interacting protein kinase 1 are critical for apoptosis signal-regulating kinase 1-JNK/p38 activation. *J Biol Chem* 2005; **280**:15061-15070.
24 Komuro Y, Takeda K, Ichijo H. Regulatory mechanism of cell death through ASK1. *Seikagaku* 2004; **76**:1458-1462.
25 Husbeck B, Stringer DE, Gerner EW, Powis G. Increased thioredoxin-1 inhibits SSAT expression in MCF-7 human breast cancer cells. *Biochem Biophys Res Commun* 2003; **306**:469-475.
26 Byun HS, Cho EW, Kim JS, *et al*. Thioredoxin overexpression in HT-1080 cells induced cellular senescence and sensitization to gamma radiation. *FEBS Lett* 2005; **579**:4055-4062.
27 Akay C, Gazitt Y. Arsenic trioxide selectively induces early and extensive apoptosis via the APO2/caspase-8 pathway engaging the mitochondrial pathway in myeloma cells with mutant p53. *Cell Cycle* 2003; **2**:358-368.
28 Choi YJ, Park JW, Suh SI, *et al*. Arsenic trioxide-induced apoptosis in U937 cells involve generation of reactive oxygen species and inhibition of Akt. *Int J Oncol* 2002; **21**:603-610.
29 Weichsel A, Gasdaska JR, Powis G, Montfort WR. Crystal structures of reduced, oxidized, and mutated human thioredoxins: evidence for a regulatory homodimer. *Structure* 1996; **4**:735-751.
30 Powis G, Wipf P, Lynch SM, Birmingham A, Kirkpatrick DL. Molecular pharmacology and antitumor activity of palmarumycin-based inhibitors of thioredoxin reductase. *Mol Cancer Ther* 2006; **5**:630-636.
31 Nguyen P, Awwad RT, Smart DD, Spitz DR, Gius D. Thioredoxin reductase as a novel molecular target for cancer therapy. *Cancer Lett* 2006; **236**:164-174.
32 Lin S, Del Razo LM, Styblo M, Wang C, Cullen WR, Thomas DJ. Arsenicals inhibit thioredoxin reductase in cultured rat hepatocytes. *Chem Res Toxicol* 2001; **14**:305-311.
33 Chouchane S , Snow ET. *In vitro* effect of arsenical compounds on glutathione-related enzymes. *Chem Res Toxicol* 2001; **14**:517-522.
34 Lu J, Chew EH, Holmgren A. Targeting thioredoxin reductase is a basis for cancer therapy by arsenic trioxide. *Proc Natl Acad Sci USA* 2007; **104**:12288-12293.
35 Masutani H, Ueda S, Yodoi J. The thioredoxin system in retroviral infection and apoptosis. *Cell Death Differ* 2005; **12** Suppl 1:991-998.
36 Powis G, Mustacich D, Coon A. The role of the redox protein thioredoxin in cell growth and cancer. *Free Radic Biol Med* 2000; **29**:312-322.
37 Kowaltowski AJ, Castilho RF, Vercesi AE. Mitochondrial permeability transition and oxidative stress. *FEBS Lett* 2001; **495**:12-15.
38 Burkitt MJ , Wardman P. Cytochrome C is a potent catalyst of dichlorofluorescin oxidation: implications for the role of reactive oxygen species in apoptosis. *Biochem Biophys Res Commun* 2001; **282**:329-333.
39 Balmer Y, Vensel WH, Tanaka CK, *et al*. Thioredoxin links redox to the regulation of fundamental processes of plant mitochondria. *Proc Natl Acad Sci USA* 2004; **101**:2642-2647.
40 Ueda S, Masutani H, Nakamura H, Tanaka T, Ueno M, Yodoi J. Redox control of cell death. *Antioxid Redox Signal* 2002; **4**:405-414.
41 Chen Q, Takeyama N, Brady G, Watson AJ, Dive C. Blood cells with reduced mitochondrial membrane potential and cytosolic cytochrome C can survive and maintain clonogenicity given appropriate signals to suppress apoptosis. *Blood* 1998; **92**:4545-4553.
42 Chen Q, Chai YC, Mazumder S, *et al*. The late increase in intracellular free radical oxygen species during apoptosis is associated with cytochrome c release, caspase activation, and mitochondrial dysfunction. *Cell Death Differ* 2003; **10**:323-334.
43 Lei X, Chen Y, Du G, *et al*. Gossypol induces Bax/Bak-independent activation of apoptosis and cytochrome c release via a conformational change in Bcl-2. *FASEB J* 2006; **20**:2147-2149.
44. Chen Q, Gong B, Almasan A. Distinct stages of cytochrome c release from mitochondria: evidence for a feedback amplification loop linking caspase activation to mitochondrial dysfunction in genotoxic stress induced apoptosis. *Cell Death Differ* 2000; **7**:227–233.
45 Chen Q, Turner J, Watson A J, Dive C. v-Abl protein tyrosine kinase (PTK) mediated suppression of apoptosis is associated with the up-regulation of BcL-XL. *Oncogene* 1997; **15**:2249–2254.
46 He TC, Zhou S, da Costa LT, Yu J, Kinzler KW, Vogelstein B. A simplified system for generating recombinant adenoviruses. *Proc Natl Acad Sci USA* 1998; **95**:2509-2514.
47 Henderson B, Tabona P, Poole S, Nair SP. Cloning and expression of the Actinobacillus actinomycetemcomitans thioredoxin (trx) gene and assessment of cytokine inhibitory activity. *Infect Immun* 2001; **69**:154-158.
48 Bernardi P. Modulation of Ca^{2+} efflux and rebounding Ca2+ transport in rat liver mitochondria. *Biochim Biophys Acta* 1984; **766**:277-282.
49 Shimizu S, Eguchi Y, Kamiike W, *et al*. Bcl-2 prevents apoptotic mitochondrial dysfunction by regulating proton flux. *Proc Natl Acad Sci USA* 1998; **95**:1455-1459.

50 Xia T, Jiang C, Li L, Wu C, Chen Q, Liu SS. A study on permeability transition pore opening and cytochrome c release from mitochondria, induced by caspase-3 *in vitro*. *FEBS Lett* 2002; **510**:62-66.
51 Narita M, Shimizu S, Ito T, *et al*. Bax interacts with the permeability transition pore to induce permeability transition and cytochrome c release in isolated mitochondria. *Proc Natl Acad Sci USA* 1998; **95**:14681-14686.
52 Inoue T, Yoshida Y, Nishimura M, Kurosawa K, Tagawa K. Ca(2+)-induced, phospholipase-independent injury during reoxygenation of anoxic mitochondria. *Biochim Biophys Acta* 1993; *1140*:313-320.
53 Rigobello MP, Donella-Deana A, Cesaro L, Bindoli A. Isolation, purification, and characterization of a rat liver mitochondrial protein disulfide isomerase. *Free Radic Biol Med* 2000; *28*:266-272.
54 Bejma J , Ji LL. Aging and acute exercise enhance free radical generation in rat skeletal muscle. *J Appl Physiol* 1999; **87**:465-470.
55 Catisti R , Vercesi AE. The participation of pyridine nucleotides redox state and reactive oxygen in the fatty acid-induced permeability transition in rat liver mitochondria. *FEBS Lett* 1999; **464**:97-101.
56 Li Y, Liu W, Xing G, Tian C, Zhu Y, He F. Direct association of hepatopoietin with thioredoxin constitutes a redox signal transduction in activation of AP-1/NF-kappaB. *Cell Signal* 2005; **17**:985-996.